POLITECNICO DI TORINO
Repository ISTITUZIONALE

Voltage-Controlled and Input-Matched Tunable Microstrip Attenuators Based on Few-Layer Graphene

(Article begins on next page)

24 April 2024

Voltage-Controlled and Input-Matched Tunable Microstrip Attenuators Based on Few-Layer Graphene

Muhammad Yasir, *Student member, IEEE*, Silvia Bistarelli, Antonino Cataldo,
Maurizio Bozzi*, Fellow, IEEE*, Luca Perregrini, *Fellow, IEEE*, and Stefano Bellucci

Abstract—This paper presents novel tunable microstrip attenuators based on few-layer graphene. The proposed topology consists of a microstrip line sided by pairs of grounded metal vias, with graphene pads located between the microstrip line and the vias. The possibility to control the graphene resistance through an applied bias voltage is exploited with the aim to modify the insertion loss of the attenuators. Several pairs of metal vias are adopted to achieve large tuning range, good input matching, and broadband operation. A systematic investigation of the structure with two, three, and four pairs of vias is presented, along with experimental validation. Prototypes operating in the frequency range from 1 GHz to 10 GHz and with maximum insertion loss exceeding 60 dB are fabricated and tested.

Index Terms— Graphene, microstrip lines, tunable microwave devices, voltage-controlled attenuator.

Fig. 1. Geometry of the graphene-based tunable microstrip attenuator proposed in [7].

I. INTRODUCTION

THE INTERESTING ELECTRONIC PROPERTIES of graphene have got significant attention in the recent years, due to the extraordinary electrical and mechanical features [1]-[3]. In the microwave frequency range, graphene exhibits the property of changing its resistance upon the application of an electric field [4]-[13]. Along with other materials (e.g., [14], [15]), the graphene represents an excellent candidate for developing microwave tunable devices. In particular, the voltage-controlled change in resistance was exploited to develop microstrip attenuators [6]-[7]. The change in graphene resistance on the application of a gate voltage was also experimentally demonstrated [8]. Moreover, the graphene tunable resistance was applied to the development of absorbers [9]-[10], phase shifters [11], and antennas [12]-[13].

Depending on the technological fabrication process, graphene for microwave applications can be realized in the form of a single layer or multiple layers [16]-[18]. Single layer graphene is technologically demanding, but on the other hand the tunable resistance characteristics of graphene are also
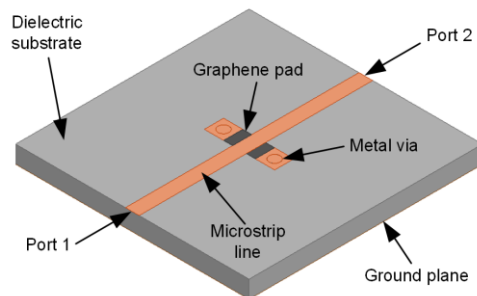
present in multilayer graphene, up to ten-layer configuration [2]. This latter property makes multilayer graphene a very good contender for use in cheap electronic and microwave circuits and systems. A cost effective and very fast method to obtain multilayer graphene was proposed in [6], [18]. This is a two-step process, which involves the microwave irradiation of intercalated graphite and a subsequent ultrasound treatment in isopropyl alcohol.

In this paper, the tunability of graphene resistance at microwave frequency and the low-cost fabrication process of multilayer graphene are combined to implement a novel class of voltage-controlled and input-matched tunable microstrip attenuators. A first implementation of a tunable microstrip attenuator based on multilayer graphene was presented in [6]. The attenuator comprised of a microstrip line with a gap, where the graphene was deposited, thus resulting in a line with a series variable resistor. A change in the graphene resistance was used to vary the attenuation of the signal between the two ports, achieving an insertion loss ranging from 5.5 dB to 10 dB at the frequency of 10 GHz. Subsequently, an improved version of graphene attenuator was developed [7]. This structure consisted of a microstrip line with two grounded vias, and the graphene was deposited in the gaps between the grounded vias and the microstrip line, as shown in Fig. 1. This structure behaves as a line with two shunt resistors, and increasing their conductivity leads to diverting the signal to ground, thus increasing the insertion loss. The achieved insertion loss ranged from 0.3 dB to 15 dB at the frequency of 3 GHz, but a large portion of the attenuation was due to reflection loss.
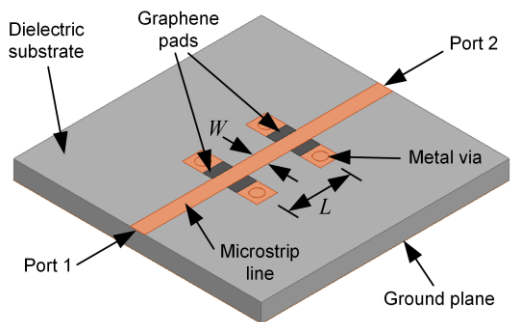
Fig. 2. Geometry of the two-pair posts tunable attenuator.

The use of multiple pairs of grounded vias with graphene in the gaps between the vias and the microstrip line allows to solve the problem of the input mismatch, along with the possibility to extend the tuning range of the insertion loss and to broaden the operation frequency band. Preliminary and partial results of this study were presented in conference papers [19], [20].

In this work, a thorough investigation of the performance of graphene attenuators is presented. The use of multiple pairs of grounded vias with graphene in the gaps between the vias and the microstrip line is considered, and a systematic parametric study is presented. The possibility to achieve large tuning range and good input matching is investigated in detail. Experimental validation is proposed for optimized configurations, in the case of two, three, and four pairs of metal vias.

II. Conduction Mechanism in Few Layer Graphene Regions

For a theoretical description of the conduction mechanism in the graphene nanoplatelets region in posts of the attenuator, the random *RCD* network model can be used [21], [22]. This model is based on a ternary network in which the basic elements depend on the composition and geometry of the regions. The first element, i.e. the resistor *R*, derives from conducting regions where agglomerates of nanocarbon are present. The second element is a capacitor *C*, coming from dielectric regions where the dielectric materials is the air between graphene flakes. The third and last element is a diode *D*, arising from hopping regions where well-dispersed nanographene particles generate hopping conductivity. These regions are randomly dispersed in graphene pads.

For a complete understanding of the process, it is possible to imagine different filling steps of the gap with increasing density of the drop casted graphene nanoplatelets, as the solvent (isopropyl alcohol) progressively evaporates, thus forming the deposit in the gap. At the beginning of the graphene nanoplatelets deposition process, only regions disconnected from each other are present. However, as the solvent's evaporations proceeds, an increasing number of previously distinct regions will approach each other until, in the end of the evaporation, a conductive network is created. The deposit in the gap is so constituted by a network of

nanostructures, i.e. the graphene nanoplatelets, each of them being several micrometers wide (see Fig. 1(*a*) in [23]). and having a crystalline structure made of stacks of 4-10 atomic layers of graphene (see Fig. 1(*b*) in [23]). The contact between the different regions is electrostatic, which is why the applicable bias between the graphene pads has a maximum value above which the circuit physically breaks [6].

In the *RCD* model, this break is associated with a disconnection of the conductive network. The graphene nanoplatelets are electrically connected by electrostatic interactions (π-π). Hence, by changing the resistivity of the graphene region, it may happen that the relative positions of the overlapping layer would be not spatially permanent. This may explain the appearing of a breakdown voltage in earlier devices, e.g. [6].

An interesting development might rely in the onset or presence of graphene-oxide. Indeed, it could happen that the graphene nanoplatelets sample could be contaminated by the graphene oxide, which in turn could enhance the oxygen-atom corrosion resistance, thus changing the conductivity response. There are important papers on the issue (e.g., [24]). On the other hand, the presence of oxidated graphene in the samples we use has been excluded by earlier characterizations [25].

III. Two-Pair Posts attenuator

The two-pair posts attenuator is composed of two couples of grounded vias, located at the sides of the microstrip line, as shown in the Fig. 2.

All attenuators presented in this work were implemented on a Taconic RF-60 substrate, with thickness h=0.64 mm, relative dielectric permittivity ε_r=6.15, and loss tangent $\tan\delta$=0.0028. The width of the input/output microstrip lines was set at 0.94 mm, in order to have a characteristic impedance of 50 Ω. Where not otherwise stated, the grounded vias have a diameter of 1.00 mm, the top metal patch is a square with side length of 1.40 mm, and the graphene pad is a rectangle with dimensions 1.40 mm by 0.66 mm. These dimensions were obtained along the lines of [7]. The commercial FEM software Ansys HFSS was adopted to perform simulations and parametric analyses of the proposed structures. Graphene was modelled as an infinitely thin resistive sheet, as discussed in [7].

In the case of two pairs of graphene pads, the distance L between the two pairs and the width W of the central microstrip section affect the insertion loss and operation bandwidth. For this reason, three different values for the distance L were analyzed in Fig. 3. Since the frequency band of operation ranges from 1 GHz to 10 GHz, the values of length L were chosen as 5 mm, 10 mm, and 15 mm, which correspond to approximately λ/6, λ/3, and λ/2, respectively, at the center frequency of 5 GHz. In order to observe the impact of the distance L on the attenuator performance, different values of graphene resistance were considered in the simulation, all falling in the range of the actual graphene resistance. It is observed in Fig. 3 that decreasing the graphene resistance leads to a larger insertion loss, ranging from 1.5 dB to more than 30 dB. Conversely, the input matching tends to degrade when decreasing the graphene resistance. Moreover, the shortest distance L=5 mm provides a flatter and quasi ripple-free transmission over the entire frequency band.
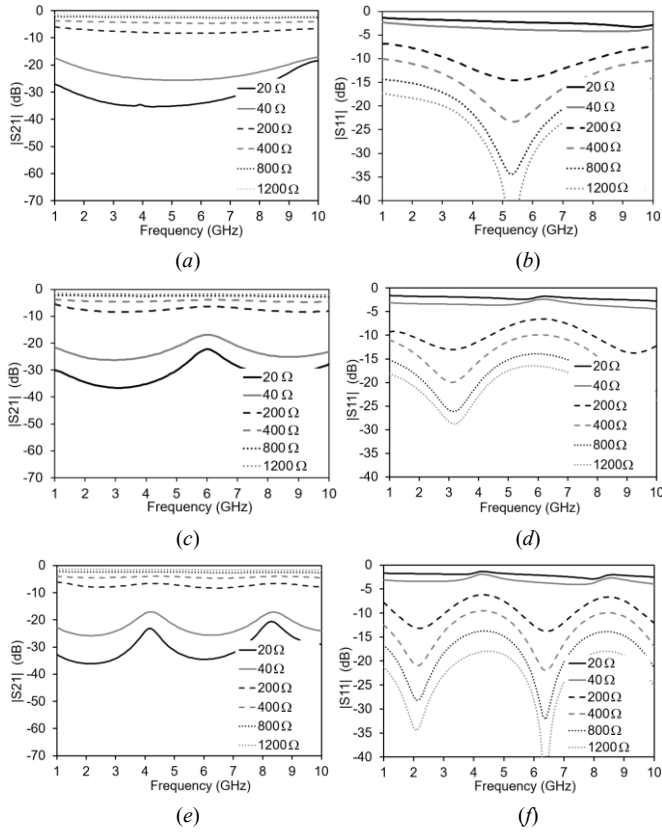
Fig. 3. Parametric simulations of the two-pair posts attenuator with variation of the midline length L (with W=940 μm): (a) $|S_{21}|$ with L=5 mm; (b) $|S_{11}|$ with L=5 mm; (c) $|S_{21}|$ with L=10 mm; (d) $|S_{11}|$ with L=10 mm; (e) $|S_{21}|$ with L=15 mm; (f) $|S_{11}|$ with L=15 mm.

Fig. 4. Parametric simulations of the two-pair posts attenuator with variation of the midline width W (with L=5 mm): (a) $|S_{21}|$ with W=940 μm (50 Ω); (b) $|S_{11}|$ with W=940 μm; (c) $|S_{21}|$ with W=630 μm (75 Ω); (d) $|S_{11}|$ with W=630 μm; (e) $|S_{21}|$ with W=470 μm (100 Ω); (f) $|S_{11}|$ with W=470 μm.

The other considered optimization parameter was the width W of the central microstrip section. The outer parts of the transmission line could not be different from 50 Ω to ensure matched connection to the ports. Three different values of width W equal to 940 μm, 630 μm, and 470 μm were analyzed, corresponding to characteristic impedance of 50 Ω, 75 Ω, and 100 Ω, respectively. The scattering parameters for all cases are shown in Fig. 4. The thickness of the central microstrip line has a minimal impact on the performance of the attenuator, the only effect being a slight increase in the insertion loss when W becomes smaller (while keeping the dynamic range constant), along with a minor degradation of the input matching. Since it is desirable to minimize the minimum insertion loss and to maximize the input matching, the optimum value is W=940 μm (50-Ω line).

Based on the results of the parametric analysis, a prototype of the two-pair posts attenuator was fabricated with the optimized values L=5 mm and W=940 μm.

The planar circuitry was realized by using an LPKF milling machine, and the vias were metalized by conductive paste. Graphene flakes were subsequently deposited as discussed in [6]. A photograph of the prototype is shown in Fig. 5(a), together with the measurement setup.
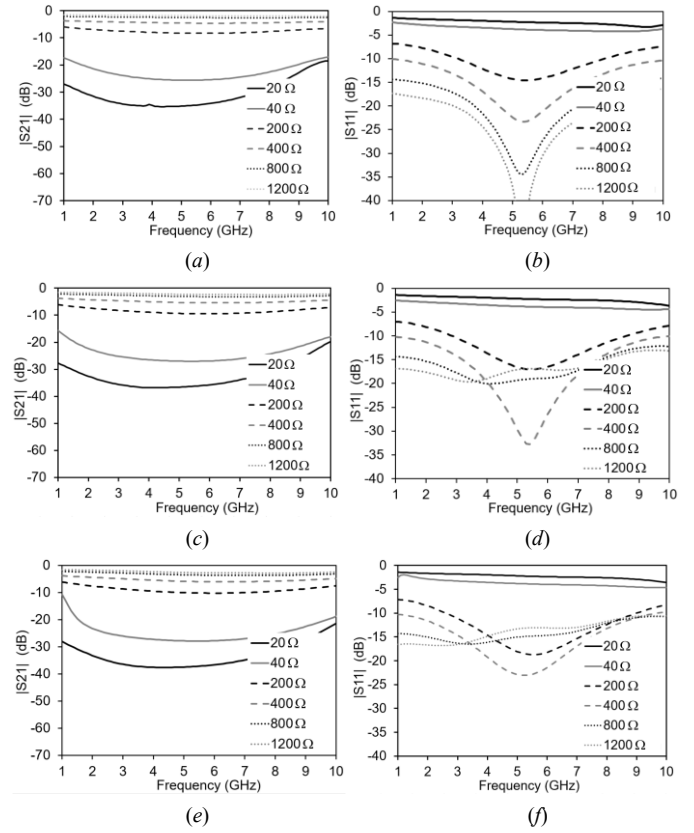
The graphene resistance was preliminarily measured, by applying the desired bias voltage and measuring the corresponding DC current. The measured DC current is equally divided into the four grounded vias, which are in parallel at DC. Table I shows the applied bias voltage V_{bias}, the DC current I_{dc} flowing across each graphene pad, and the resulting equivalent resistance $R=V_{bias}/I_{dc}$ of the single graphene pad. As expected, the resistance R decreases when increasing the applied bias voltage.

RF measurements were carried out with a vector network analyzer, and the graphene was biased by using a bias-tee [Fig. 5(a)]. The variation of the graphene resistance versus the bias voltage allows controlling the insertion loss of the

TABLE I – GRAPHENE RESISTANCE OF THE TWO-PAIR POSTS ATTENUATOR

V_{bias} (V)	I_{dc} (A)	R (Ω)
0	===	1550*
3.5	0.0085	410
4	0.016	250
5.5	0.119	46

* Measured by using a multimeter.
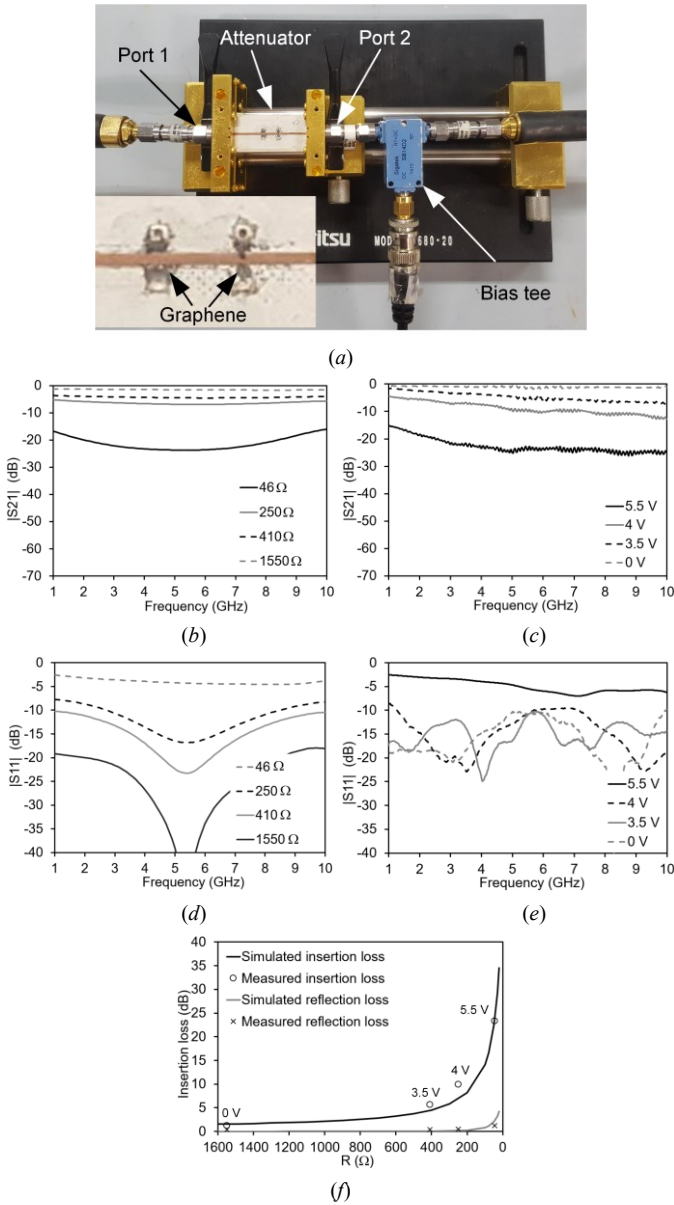
(a)

(b)

(c)

(d)

(e)

(f)

Fig. 5. Experimental verification of the two-pair posts graphene attenuator: (a) Photograph of the prototype; (b) Simulated transmission; (c) Measured transmission; (d) Simulated reflection; (e) Measured reflection; (f) Simulated and measured insertion loss at 6 GHz.

Fig. 6. Geometry of the three-pair posts tunable attenuator.

insertion loss at 6 GHz ranges from 1.2 dB at V_{bias}=0 to 24 dB at V_{bias}=5.5 V. The reflection loss does not exceed the value of 4 dB at V_{bias}=5.5 V. The maximum value of bias voltage is determined by the breakdown of the device [6].

IV. THREE-PAIR POSTS ATTENUATOR

An increased number of pairs of graphene pads with grounded vias was adopted to achieve a higher insertion loss and to improve the input matching. In the second structure, the number of pairs was increased to three (Fig. 6).

As a baseline, all design parameters were kept identical to the attenuator with two pairs of posts, discussed in the previous section. In this section, the effect of the dimensions of the graphene pads g_1, g_2, and g_3 on the transmission scattering parameters is analyzed. For sake of symmetry, the dimension of the outer graphene pads is kept identical, with g_1=g_3.

In the first parametric study, the dimension g_2 of the inner graphene pad was varied (Fig. 7), considering the nominal value (g_2=660 μm) and reductions to 70% (g_2=462 μm) and to 40% (g_2=264 μm). As shown in Fig. 7, the decrease in g_2 results in an increase of the insertion loss, both in the maximum value (desirable) and in the minimum value (highly undesired). Moreover, decreasing g_2 has a detrimental effect on the input matching.

In the second parametric study, the same variation was applied to the dimensions g_1=g_3 of the outer graphene pads. The results in terms of the scattering parameters are as shown in the Fig. 8. The impact of the outer pads size reduction is similar to the inner one, resulting into an increase of both minimum and maximum insertion loss and a degradation of the input matching. In this case, the performance degradation is even more pronounced, as it involves two pairs of graphene pads (the outer ones) instead of one (the inner one).

Based on the parametric analyses, the dimensions g_1=g_2=g_3=660 μm was adopted for the final prototype. The prototype of the attenuator with three pairs of graphene pads was fabricated, and its picture is shown in Fig. 9(a).

The measurement setup adopted for the DC and RF measurements is identical to the one described in Sec. II and shown in Fig. 5(a).

attenuator. When increasing the DC bias voltage, the resistance of graphene reduces, thus increasing the insertion loss. Figs. 5(b)-5(e) show the scattering parameters of the attenuator obtained from measurements (with different values of bias voltage V_{bias}) and from simulations (performed with the corresponding values of graphene resistance R, see Table I). In the frequency range from 3 GHz to 10 GHz, the measured insertion loss ranges from a low value of 1.2±0.6 dB at zero bias voltage to a high value of 24±2 dB at a bias voltage of 5.5 V.

A clear summary of the attenuator performance at the central frequency of 6 GHz is provided in Fig. 5(f), which shows the simulated and measured total insertion loss as well as the portion of insertion loss due to reflection. The total
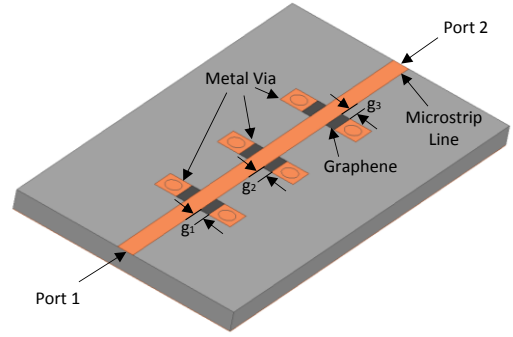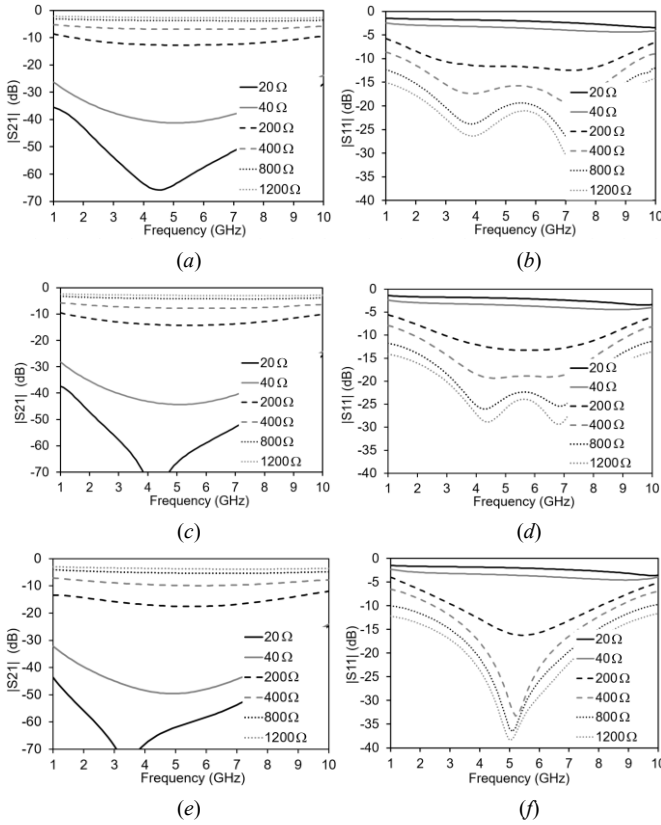
Fig. 7. Parametric simulations of the three-pair posts attenuator with variation of the inner graphene pad dimension g_2, with $g_1=g_3=660$ μm: (a) $|S_{21}|$ with $g_2=660$ μm; (b) $|S_{11}|$ with $g_2=660$ μm; (c) $|S_{21}|$ with $g_2=462$ μm; (d) $|S_{11}|$ with $g_2=462$ μm; (e) $|S_{21}|$ with $g_2=264$ μm; (f) $|S_{11}|$ with $g_2=264$ μm.

Fig. 8. Parametric simulations of the three-pair posts attenuator with variation of the outer graphene pad dimensions $g_1=g_3$, with $g_2=660$ μm: (a) $|S_{21}|$ with $g_1=g_3=660$ μm; (b) $|S_{11}|$ with $g_1=g_3=660$ μm; (c) $|S_{21}|$ with $g_1=g_3=462$ μm; (d) $|S_{11}|$ with $g_1=g_3=462$ μm; (e) $|S_{21}|$ with $g_1=g_3=264$ μm; (f) $|S_{11}|$ with $g_1=g_3=264$ μm.

As a first step, the graphene resistance was measured, for different values of bias voltage. Table II shows the applied bias voltage V_{bias}, the measured DC current I_{dc} flowing across each graphene pad, and the equivalent resistance R of the single graphene pad.

Subsequently, RF measurements were performed, and the comparison between simulations and measurements of the scattering parameters are shown in Figs. 9(b)-9(e). Also in this case, the resistance values adopted in the simulations correspond to the applied bias voltage used in the measurements, according to the results of Table II. In the frequency range from 3 GHz to 10 GHz, the measured insertion loss ranges from a low value of 1.7±0.9 dB at zero bias voltage to a high value of 32±4 dB at a bias voltage of 6 V.

A summary of the attenuator performance at the central frequency of 6 GHz is provided in Fig. 9(f), which shows the simulated and measured total insertion loss as well as the portion of insertion loss due to reflection. The structure with three pairs of graphene pads provides a larger value of maximum insertion loss, while preserving low minimum insertion loss and good input matching. In particular, at the central frequency of 6 GHz, the maximum measured insertion loss in this case is around 33 dB with a bias voltage of 6 V, the minimum insertion loss is 1.2 dB for 0 V, and the reflection loss does not exceed the value of 1.1 dB at 6 V.

V. FOUR-PAIR POSTS ATTENUATOR

An attenuator based on four pairs of graphene pads and grounded vias was designed and fabricated, based on the parametric analyses presented in the previous sections. The aim of this last structure is to achieve maximum range of insertion loss with minimum degradation of the input matching, over the frequency band from 1 GHz to 10 GHz.

The proposed design of four-pairs post attenuator is as shown in the Fig. 10, where the dimensions coincide with the optimal values derived from the parametric analyses (L=5 mm, W=0.94 mm, s=1.40 mm, and g=0.66 mm). A photograph of the prototype is shown in the Fig. 11(a).

TABLE II – GRAPHENE RESISTANCE VERSUS VOLTAGE FOR THE THREE-PAIR POSTS ATTENUATOR

V_{bias} (V)	I_{dc} (A)	R (Ω)
0	===	1443[*]
2	0.0021	950
4	0.0139	286
6	0.1052	57

[*] Measured by using a multimeter.

(a)

(b)

(c)

(d)

(e)

(f)

Fig. 9. Experimental verification of the three-pair posts graphene attenuator: (a) Photograph of the prototype; (b) Simulated transmission; (c) Measured transmission; (d) Simulated reflection; (e) Measured reflection; (f) Simulated and measured insertion loss at 6 GHz.
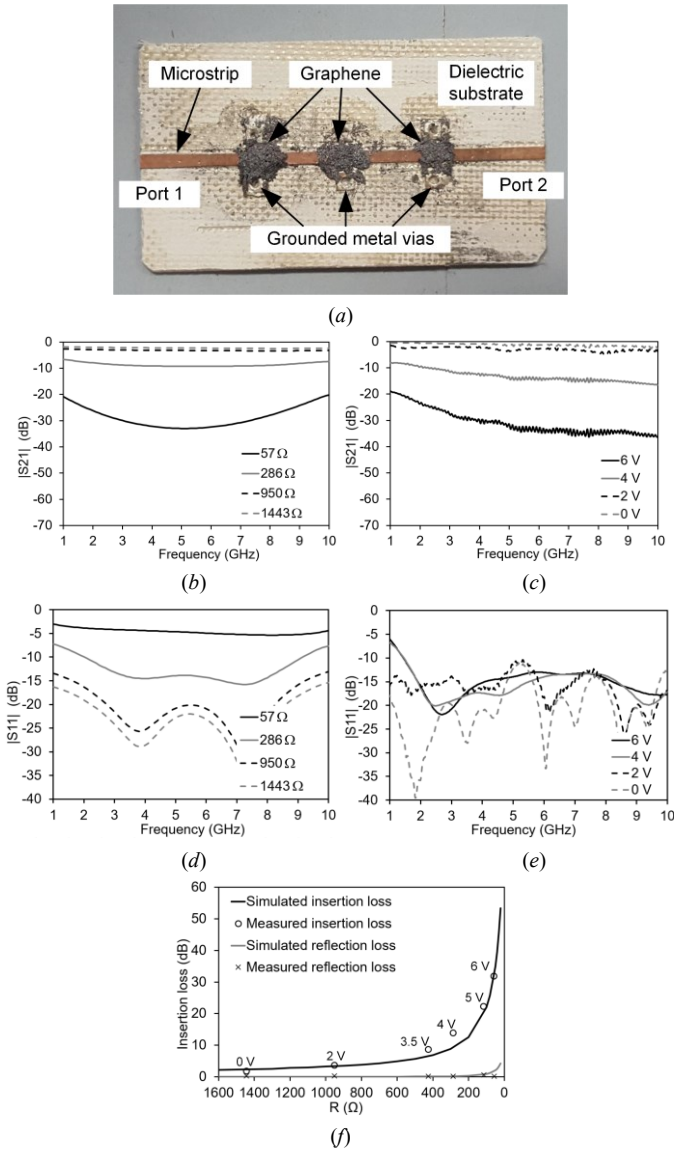
Measurements of the prototype were performed as in the other two cases. Preliminary DC measurements allow to obtain the graphene resistance as a function of the applied bias voltage, as shown in Table III. The comparison of simulations and RF measurements is provided in Figs. 11(b)-11(e), where the simulated scattering parameters obtained with different values of graphene resistance are compared with measured results achieved with the corresponding values of bias voltage (Table III). The use of four pairs of graphene pads allows to achieve a very large dynamic range of the insertion loss. The measured insertion loss is larger than 48 dB in the frequency band from 3 GHz to 10 GHz with a bias voltage of 7 V, and the minimum insertion loss (at zero bias voltage) ranges from 1.2 dB at 3 GHz to 3.9 dB at 10 GHz. The input matching is better than 5 dB in the same frequency band.
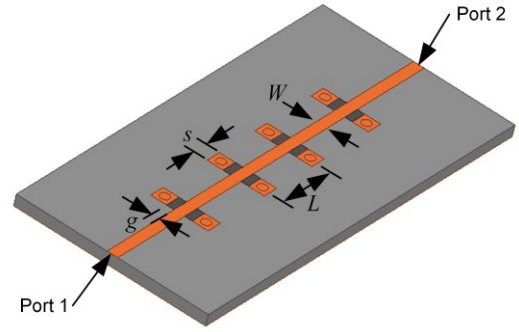

Fig. 10. Geometry of the four-pair posts tunable attenuator.

The simulated and measured total insertion loss and the portion of insertion loss due to reflection are shown in Fig. 11(f). At the frequency of 6 GHz, the attenuation loss is 59 dB where the insertion loss due to reflection does not exceed the value of 2.3 dB.

VI. DISCUSSION AND COMPARISON WITH STATE-OF-THE-ART

The comparison of the different solutions proposed in this paper shows that increasing the number of pairs of graphene pads allows to extend the dynamic range of the insertion loss and to reduce the reflection loss.

The basic principle of operation of the proposed tunable attenuator can be easily understood by adopting the equivalent circuit model shown in Fig. 12(a), where each pair of graphene pads, connected to ground by shorting vias, is represented by a resistor connected to ground. Fig. 12 also shows the circuit-based simulation results for different cases: more specifically, it reports the scattering parameters of the attenuators with one pair [Figs. 12(b) and 12(c)], two pairs [Figs. 12(d) and 12(e)], three pairs [Figs. 12(f) and 12(g)], and four pairs [Figs. 12(h) and 12(i)] of graphene pads, for different values of graphene resistance. The results shown in Fig. 12 demonstrate that, by increasing the number of pairs of graphene pads, there are additional degrees of freedom in the structure and this allows to increase significantly both the bandwidth of the input matching and the dynamic range of the insertion loss.

Finally, to better appreciate this behavior, Fig. 13 shows the total insertion loss and the reflection loss versus the bias voltage for all three attenuators presented in this paper and the single-pair attenuator proposed in [7]. The attenuation is measured at the central operation frequency, which is 6 GHz for the attenuators with two-, three-, and four-pair posts, and 3 GHz for the single-pair post attenuator in [7].

TABLE III – GRAPHENE RESISTANCE VERSUS VOLTAGE FOR THE FOUR-PAIR POSTS ATTENUATOR

V_{bias} (V)	I_{dc} (A)	R (Ω)
0	===	1347*
3	0.0057	526
4	0.0149	267
5	0.063	79
7	0.189	37

* Measured by using a multimeter.
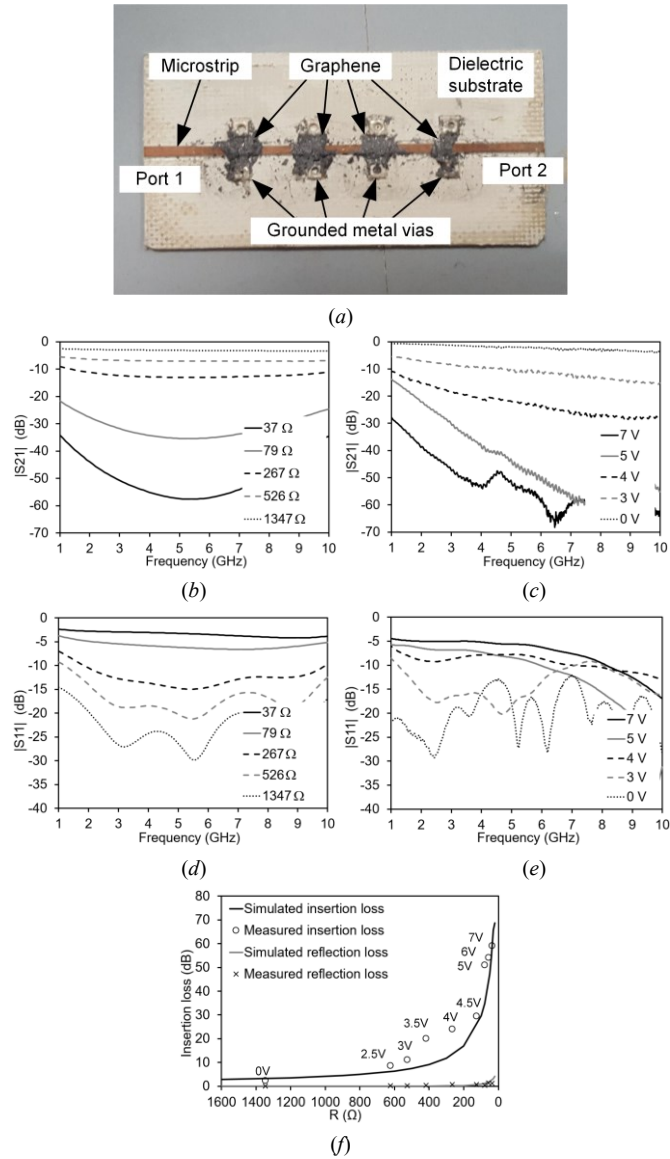
(a)

(b)

(c)

(d)

(e)

(f)

Fig. 11. Experimental verification of the four-pair posts graphene attenuator: (a) Photograph of the prototype; (b) Simulated transmission; (c) Measured transmission; (d) Simulated reflection; (e) Measured reflection; (f) Simulated and measured insertion loss at 6 GHz.

(a)

(b)

(c)

(d)

(e)

(f)

(g)

(h)

(i)

Fig. 12. Analysis of the graphene-based attenuator with different number of pairs of graphene pads, based on the equivalent circuit model: (a) Topology of the equivalent circuit model; (b) Simulated $|S_{11}|$ for one pair of graphene pads; (c) Simulated $|S_{21}|$ for one pair of graphene pads; (d) Simulated $|S_{11}|$ for two pairs of graphene pads; (e) Simulated $|S_{21}|$ for one pair of graphene pads; (f) Simulated $|S_{11}|$ for three pairs of graphene pads; (g) Simulated $|S_{21}|$ for one pair of graphene pads; (h) Simulated $|S_{11}|$ for four pairs of graphene pads; (i) Simulated $|S_{21}|$ for one pair of graphene pads.

When using one single pair of graphene pads, the maximum achievable insertion loss is 15 dB, out of which 4 dB are attributed to reflection loss. Increasing the number of pairs to two results in a maximum insertion loss of 23 dB, and only 1.2 dB reflection loss. Using an even larger number of pairs allows extending the maximum insertion loss (up to more than 58 dB with four-pair posts), while keeping the reflection loss below 1.3 dB.

In the proposed solutions, the insertion loss is mainly due to dissipation, and the reflection is a very small portion of the total attenuation. Nevertheless, a reflection loss of 1.3 dB corresponds to an input matching of approximately 6 dB, which may be not enough for some applications. Of course, a better input matching can be achieved by limiting the bias voltage to lower values, with the effect to cap the maximum insertion loss.

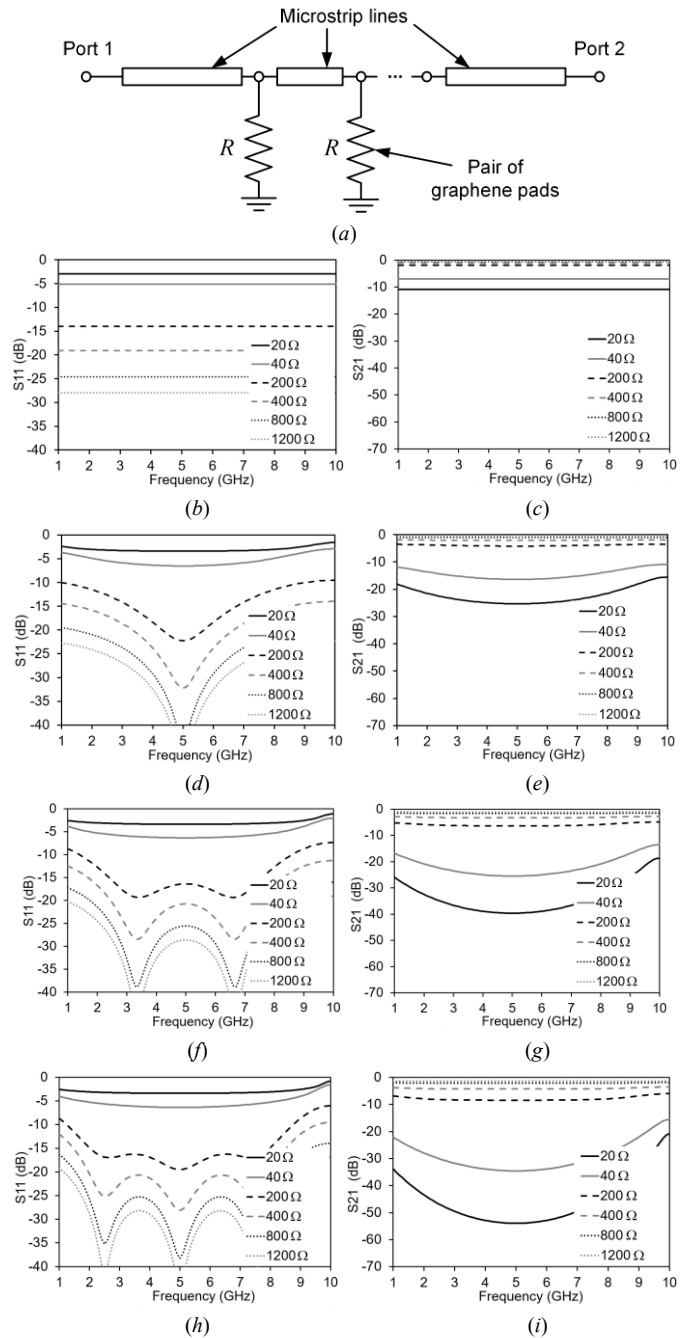However, in the case of the three-pair posts attenuator, the reflection loss is below 0.5 dB over the frequency band from 3 GHz to 10 GHz, which corresponds to an input matching of 10 dB. In this frequency range, this attenuator is able to reach an insertion loss larger than 30 dB.
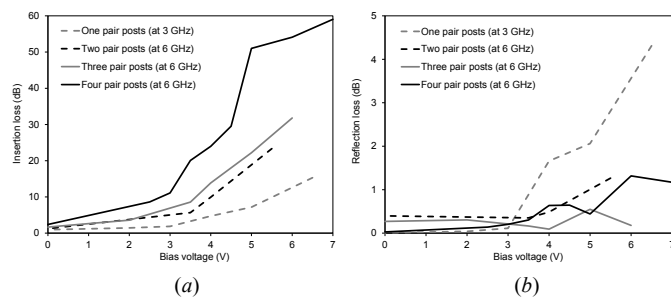
Fig. 13. Comparison of the graphene-based attenuators with different number of pairs of graphene pads: (*a*) Total insertion loss vs. the bias voltage at the center frequency; (*b*) Reflection loss vs. the bias voltage at the center frequency.

In order to locate the proposed solutions in the framework of the current state-of-the-art attenuators based on graphene technology, several recent papers on graphene attenuators are considered [26]-[28]. Table IV summarizes the key performance of the structures presented in the literature and of the three attenuators based on graphene proposed in this work. Compared with the state-of-the-art, the proposed attenuator exhibits a much larger value of maximum insertion loss, a slightly better value of minimum insertion loss, and a more limited input matching. The relative frequency band is comparable with the best cases proposed in the literature.

VII. CONCLUSION

This paper has presented a set of voltage-controlled microstrip attenuators based on graphene technology. The cost-effective technology of few-layer graphene has been adopted for the fabrication of the attenuators. The proposed topology, based on multiple pairs of graphene pads located between the microstrip and grounded vias exhibits significant potential to achieve large values of insertion loss, while minimizing the reflection loss. Prototypes operating in the frequency band from 1 GHz to 10 GHz have been shown, outperforming the state-of-the-art in graphene attenuators in terms of maximum and minimum insertion loss. The limited accuracy in the deposition of graphene could slightly modify the electrical performance of the circuit. Nonetheless, the current accuracy is sufficient to show the physical effect and applicability at tunable microwave devices and to demonstrate the proper operation of the proposed device.

TABLE IV – COMPARISON OF GRAPHENE-BASED ATTENUATORS

	Min insertion loss (dB)	Max insertion loss (dB)	Max $|S_{11}|$ (dB)	Frequency band (GHz)	Bias Voltage (V)
[26]	4	16	-15	7-15	0-4
[27]	3	15	-20	7.7-19	0-4
[28]	3	15	-15	9-40	0-4
1-pair	0.3	14	-2	0-5	0-6.5
2-pairs	1.2	20	-4	3-10	0-5.5
3 pairs	2.6	30	-10	3-10	0-6
4-pairs	3.9	48	-5	3-10	0-7

REFERENCES

[1] S K.S. Novoselov *et al.*, "Electric field effect in atomically thin carbon films," *Science*, Vol. 306, No. 5696, pp. 666–669, 2004.

[2] A. H. C. Neto, F. Guinea, N. M. R. Peres, K. S. Novosolev and A. K. Giem, "The electronic properties of graphene," *Rev. Mod. Phys.*, Vol. 81, no. 1, pp. 109-162, 2009.

[3] R. Quhe *et al.*, "Tunable band gap in few-layer graphene by surface adsorption," *Scientific Reports*, Vol. 3, No. 1794, May 2013.

[4] M. Dragoman *et al.*, "Graphene for Microwave," *IEEE Microwave Magazine*, pp. 81-86, Dec. 2010.

[5] M. Bozzi, L. Pierantoni, and S. Bellucci, "Applications of Graphene at Microwave Frequencies," *Radioengineering*, Vol. 24, No. 3, pp. 661-669, Sept. 2015

[6] L. Pierantoni *et al.*, "Broadband Microwave Attenuator Based on Few Layer Graphene Flakes," *IEEE Trans. Microwave Theory Techn.*, Vol. 63, No. 8, pp. 2491-2497, Aug. 2015.

[7] M. Yasir, S. Bistarelli, A. Cataldo, M. Bozzi, L. Perregrini, and S. Bellucci, "Enhanced Tunable Microstrip Attenuator Based on Few Layer Graphene Flakes," *IEEE Microwave and Wireless Components Letters*, Vol. 27, No. 4, pp. 332-334, Apr. 2017.

[8] A. Fallahi and J. Perruisseau-Carrier, "Design of tunable biperiodic graphene metasurfaces," Phys. Rev. B, Condens. Matter, vol. 86, no. 19, p. 195408, 5, Nov. 2012.

[9] O. Balci, E. O. Polat, N. Kakenov and C. Kocabas, "Graphene enabled electrically switchable radar absorbing surfaces," *Nature Communications,* Vol. 6, p. 6628, Mar. 2015.

[10] D. Yi, X. C. Wei, Y. L. Xu, "Tunable Microwave Absorber Based on Patterned Graphene," *IEEE Transactions on Microwave Theory and Techniques*, Vol. 65, No. 8, pp. 2819-2826, Aug. 2017.

[11] M. Yasir, S. Bistarelli, A. Cataldo, M. Bozzi, L. Perregrini, and S. Bellucci, "Tunable Phase Shifter Based on Few-Layer Graphene Flakes," *IEEE Microwave and Wireless Components Letters*, Vol. 29, No. 1, pp. 47-49, Jan. 2019.

[12] C. N. Alvarez, R. Cheung, J. S. Thompson, "Performance Analysis of Hybrid Metal-Graphene Frequency Reconfigurable Antennas in the Microwave Regime," *IEEE Transactions on Antennas and Propagation*, Vol. 65, No. 4, pp. 1558-1569, Apr. 2017.

[13] M. Yasir, P. Savi, S. Bistarelli, A. Cataldo, M. Bozzi, L. Perregrini, S. Bellucci, "A Planar Antenna With Voltage-Controlled Frequency Tuning Based on Few Layer Graphene," *IEEE Antennas and Wireless Propagation letters*, Vol. 16, No. 1, pp. 2380-2383, Jun. 2017.

[14] H. Lv *et al.*, "A Voltage- Boosting Strategy Enabling a Low-Frequency, Flexible Electromagnetic Wave Absorption Device," *Advanced Functional Materials.*, Vol. 30, No. 15, pp. 1-8, Mar. 2018.

[15] H. Lv *et al.*, "A Flexible Microwave Shield with Tunable Frequency-Transmission and Electromagnetic Compatibility," *Advanced Functional Materials.*, Vol. 29, No. 14, pp. 1-8, Feb. 2019.

[16] W. A. de Heer *et al.*, "Epitaxial graphene," *Solid State Communications*, Vol.143, No. 1–2, pp. 92-100, July 2007.

[17] H. Cao *et al.*, "Electronic transport in chemical vapor deposited graphene synthesized on Cu: Quantum Hall effect and weak localization," *Applied Physics Letters*, Vol. 96, 122106, 2010.

[18] A. Dabrowska, S. Bellucci, A. Cataldo, F. Micciulla, A. Huczko, "Nanocomposites of epoxy resin with graphene nanoplates and exfoliated graphite: Synthesis and electrical properties," *Physica Status Solidi* (b), Vol. 251, pp. 2599-2602, 2014.

[19] M. Yasir, S. Bistarelli, A. Cataldo, M. Bozzi, L. Perregrini, and S. Bellucci, "Highly tunable and Large Bandwidth Attenuator based on Few layer Graphene," *International Microwave Workshop Series on Advanced Materials and Processes (IMWS-AMP)*, Pavia, Italy, Sep. 2017.

[20] M. Yasir, S. Bistarelli, A. Cataldo, M. Bozzi, L. Perregrini, and S. Bellucci, "Tunable and Input-Matched Attenuator based on Few layer Graphene," *IEEE 47th European Microwave Conference (EuMC)*, Nuremberg, Germany, Oct. 2017.

[21] D. Bychanok *et al.*, "A study of random resistor-capacitor-diode networks to assess the electromagnetic properties of carbon nanotube filled polymers," *Appl. Phys. Lett.*, vol. 103, No. 24, pp. 243104, Nov. 2013.

[22] S. Bellucci *et al*., "Broadband Dielectric Spectroscopy of Composites Filled With Various Carbon Materials," *IEEE Trans. Microwave Theory Techn.*, vol. 63, no. 6, pp. 2024-2031, June 2015.

[23] N. I. Volynets et al., "Shielding Properties of Composite Materials Based on Epoxy Resin with Graphene Nanoplates in the Microwave Frequency Range," *Tech. Phys. Lett.*, Vol. 42, No. 12, pp. 1141-1144, Dec. 2016.

[24] A. M. Dimiev and J. M. Tour. "Mechanism of graphene oxide formation," *ACS Nano*, Vol. 8, No. 3, pp. 3060-3068, Feb. 2014.

[25] A. Maffucci, F. Micciulla, A. Cataldo, G. Miano, and S. Bellucci, "Bottom-up realization and electrical characterization of a graphene-based device," *Nanotechnology*, Vol. 27, No. 9, Feb. 2016.

[26] A. Zhang, W. Lu, Z. Liu, H. Chen and B. Huang, "Dynamically Tunable Substrate-Integrated Waveguide Attenuator Using Graphene," *IEEE Trans Microwave Theory Techn.*, Vol. 66, No. 6, pp. 3081-3089, Jun. 2018.

[27] A. Zhang, Z. Liu, W. Lu, and H. Chen, "Graphene-based dynamically tunable attenuator on a half-mode substrate integrated waveguide," *Appl. Phys. Lett.*, Vol. 112, No. 1, pp. 161903, Apr. 2018.

[28] A. Zhang, Z. Liu, W. Lu and H. Chen, "Graphene-Based Dynamically Tunable Attenuator on a Coplanar Waveguide or a Slotline," *IEEE Trans Microwave Theory Techn.*, Vol. 67, No. 1, pp. 70-77, Jan. 2019.

Antonino Cataldo received his Master degree in chemistry (with a specialization in physical chemistry) from the University of Palermo, Italy, in 2011, and the Ph.D. in chemistry (working on structural and functional properties of nanocomposites) in 2015. Currently, he is a research fellow at Polytechnic University of Marche.

His experimental activities concern nanoscience of carbon materials: preparation of carbon nanotube and graphene using different techniques (CVD, microwave exfoliation); microscopic, spectroscopic, electrical and electrochemical characterization of nanomaterials; nanocomposite materials for EMI shielding, electrochemical and sensor application; microgravity effects on living cells; supramolecular chemistry for stabilization and drug delivery systems; environmental remediation; characterization of soft matter and colloidal systems with small angle scattering techniques.

From 2013 he has been a member of the local organizing committee of the international workshop "Nanoscience and Nanotechnology" in Frascati (Italy). He was involved in several national and international project, as well as NATO for peace project entitled "Development of Biosensors using Carbon Nanotubes Biosensors using Carbon Nanotubes"; Italian Ministry of Health project entitled "Delivery and imaging of miRNAs by multifunctional carbon nanotubes and circulating miRNAs as innovative therapeutic and diagnostic tools for pediatric pulmonary hypertension"; FP7 project entitled Nano-Thin And Micro-Sized Carbons: Toward Electromagnetic Compatibility Application. He co-authored more than 37 papers in international peer-reviewed journals.

Muhammad Yasir was born in Pakistan in 1990. He received his bachelors and masters degrees in Electronic Engineering from Politecnico di Torino, Italy, in 2012 and 2014, respectively. He received his PhD degree in electronics, computer science and electrical engineering from the University of Pavia, Italy, in 2019.

He was a visiting researcher in IMT Bucharest where he worked on graphene nonlinear devices for electromagnetic energy harvesting in 2018. He was a researcher at the University of Pavia from 2018 to 2019. He is currently a research fellow at the Department of Electronics and Telecommunications of Politecnico di Torino where he is working on nanomaterials applications in microwaves, antennas and sensing.

Dr. Yasir was the recipient of the best student paper award at the 16th Mediterranean Microwave Symposium (MMS 2016).

Silvia Bistarelli was born in 1988 and graduated in high school (science course) in 2007. From 2007 to 2010 she attended "La Sapienza" University of Rome and obtained her bachelor in Physics with 110/110. From 2010 to 2012 she received her master degree in Physics from "La Sapienza" University of Rome with curriculum in Matter Physics with 110/110. For her thesis, she worked at INFN-LNF (Istituto Nazionale di Fisica Nucleare-Laboratori Nazionali di Frascati), in the NEXT group directed by Dr. Stefano Bellucci, with research including carbon nanostructures and biomedical applications. In 2017, she got her PhD in "Condensed matter, nanotechnology and complex system" from "Roma Tre" University of Rome studying nanocarbon materials, including graphene, in electromagnetic shielding applications. She published over 25 papers in peer-reviewed journals.

Maurizio Bozzi (S'98–M'01–SM'12–F'18) was born in Voghera, Italy, in 1971. He received the Ph.D. degree in electronics and computer science from the University of Pavia, Pavia, Italy, in 2000.

He held research positions with various universities worldwide, including the Technische Universität Darmstadt, Germany; the Universitat de Valencia, Spain; and the École Polytechnique de Montréal, Canada. In 2002, he joined the Department of Electronics, University of Pavia, where he is currently a full professor of electromagnetic fields.

He was also a Guest Professor at Tianjin University, China (2015-2017) and a Visiting Professor at Gdansk University of Technology, Poland (2017-2018).

He has authored or co-authored more than 130 journal papers and 300 conference papers. He co-edited the book Periodic Structures (Research Signpost, 2006) and co-authored the book Microstrip Lines and Slotlines (Artech House, 2013). His main research interests concern the computational electromagnetics, the substrate integrated waveguide technology, and the use of novel materials and fabrication technologies for microwave circuits (including paper, textile, and 3D printing).

Prof. Bozzi is an Elected Member of the Administrative Committee of the IEEE Microwave Theory and Techniques Society (MTT-S) for terms 2017–2019 and 2020–2022, and the Chair of the Meeting and Symposia Committee of MTT-S AdCom for years 2018–2019. He was the Secretary of IEEE MTT-S for year 2016 and a member of the General Assembly (GA) of the European Microwave Association (EuMA) from 2014 to 2016. He is a track editor of the IEEE Transactions on Microwave Theory and Techniques. He was an associate editor of the IEEE Microwave and Wireless Components Letters, *IET Electronics Letters*, and *IET Microwaves, Antennas and Propagation*. He was the Guest Editor of special issues in the IEEE Transactions on Microwave Theory and Techniques, the IEEE Microwave Magazine, and the *IET Microwaves, Antennas and Propagation*. He was the General Chair of the IEEE MTT-S International Microwave Workshop Series-Advanced Materials and Processes (IMWS-AMP 2017), in Pavia, Italy, 2017, of the inaugural edition of the IEEE International Conference on Numerical Electromagnetic Modeling and Optimization (NEMO2014), in Pavia, Italy, 2014, and of the IEEE MTT-S International Microwave Workshop Series on Millimeter Wave Integration Technologies, in Sitges, Spain, 2011.

He received several awards, including the 2015 Premium Award for Best Paper in IET Microwaves, Antennas & Propagation, the 2014 Premium Award for the Best Paper in Electronics Letters, the Best Student Paper Award at the 2016 IEEE Topical Conference on Wireless Sensors and Sensor Networks (WiSNet2016), the Best Paper Award at the 15th Mediterranean

Microwave Symposium (MMS2015), the Best Student Award at the 4th European Conference on Antennas and Propagation (EuCAP 2010), the Best Young Scientist Paper Award of the XXVII General Assembly of URSI in 2002, and the MECSA Prize of the Italian Conference on Electromagnetics (XIII RiNEm), in 2000.

Luca Perregrini (M'97-SM'12-F'16) was born in Sondrio, Italy, in 1964. He received the Laurea degree in Electronic Engineering and the Ph.D. in Electronics and Computer Science in 1989 and 1993, respectively. In 1992 he joined the Faculty of Engineering of the University of Pavia, he is currently full professor of electromagnetic fields and responsible of the Microwave Laboratory. He has been a visiting professor at the École Polytechnique de Montréal, Québec, Canada in 2001, 2002, 2005, and 2006.

He has been responsible of many research contracts with prominent international research centers and companies. His main research interests have been focused on the development of numerical methods for electromagnetics, and the design of microwave components and antennas. He authored or co-authored more than 90 journal papers and more than 250 conference papers, six book chapters, two textbooks, and co-edited the book Periodic Structures, (Research Signpost, 2006). His current research interests include the development of numerical methods for electromagnetics, and the design of microwave components and antennas.

Prof. Perregrini has been an invited speaker at many conferences, and has delivered invited seminar talks in Universities and research centers worldwide. He was a member of the General Assembly of the European Microwave Association (EuMA) from 2011 to 2013. He is a member of the Technical Committee MTT–15 (Microwave Field Theory) of IEEE Microwave Theory and Technique Society (MTT-S), of the Board of Directors of EuMA. He served as a member of prize committees for several conferences/societies.

He is Fellow of the Institute of Electrical and Electronics Engineers (IEEE). He was the co-recipient of several the best paper awards at international conferences. He is the appointed Technical Program Committee Chair of the International Microwave Workshop Series on Advanced Materials and Processes (IMWS-AMP 2017), Pavia, Italy, in 2017. He was the Technical Program Committee Chair of the IEEE MTT-S International Conference on Numerical Electromagnetic Modeling and Optimization (NEMO2014), Pavia, Italy, in 2014, and of the European Microwave Conference, Rome, Italy, in 2014. He was Associate Editor of the IEEE Microwave and Wireless Components Letters from 2010 to 2013, of IEEE Transactions on Microwave Theory and Techniques from 2013 to 2016, of the International Journal of Microwave and Wireless Technologies from 2011 to 2016, and of IET Electronic Letters from 2015 to 2016. He was Guest Editor of the IEEE Transactions on Microwave Theory and Techniques in 2015 and of the International Journal of Microwave and Wireless Technologies in 2015. He is currently Editor in Chief of the IEEE Transactions on Microwave Theory and Techniques.

Stefano Bellucci obtained in 1982 the Laurea in Physics Degree at Univ. Sapienza Rome (summa cum laude) and in 1986 his Ph.D. in Physics of elementary particles at SISSA, Trieste. He worked as Research Associate at Brandeis Univ., Waltham, MA, USA (1983-1985); as visiting researcher at M.I.T., Cambridge, MA, USA (1985-1986), at Univ. of Maryland, USA (1986-1987), at Univ. of California at Davis, USA (1987-1988). He was appointed as a Tenured Researcher (Research Staff) at INFN (Istituto Nazionale di Fisica Nucleare) Laboratori Nazionali di Frascati (LNF) in 1987. He was appointed as INFN First Researcher (Senior Research Staff) in 2005. Italy Ministry of University in 2013 habilitated him as Full Professor in Theoretical Physics of Fundamental Interactions and in Theoretical Condensed Matter Physics. He coordinated (1999-2002, 2011-2015) all LNF theoretical physics activities. His research interests include theoretical physics, condensed matter, biophysics, physical chemistry, nanoscience and nanotechnology, nanocarbon based composites, toxicology, biomedical applications. His lab cultivated over

40 PhD and master students. He published over 550 papers with 12029 citations (4540 citations since 2014) in peer-reviewed journals with Hirsch index h = 52, and more than 10 invited book chapters,. Editor and/or co-author of over 10 books with Springer. In the list of Top Italian Scientists published by VIA Academy.

Received B.W. Lee Prize at Erice School of Subnuclear Physics (Erice, Italy) 1982. In 1980 he was selected as Summer student at CERN (Geneva). He led INFN applied physics CSN5 experiments: 2006-2010 NEXT for new electron sources and X radiation, 2004-2006 MINCE for micro and nano technology, 2001-2004 NANO for carbon-based nanotechnology. He was in 2007-2010 INFN Scientist and technologist in charge for EU FP7-ICT-2007-1 Collaborative Project CATHERINE "Carbon nAnotube Technology for Highspeed nExt-geneRation nano-InterconNEcts".

He is Series Editor of Springer Lecture Notes in Nanoscale Science and Technology, and biannual (2012-2014) Associate Editor of Nanoscience and Nanotechnology Letters. He is Editorial Board Member of and many scientific journals, e.g. the Journal of Nanomaterials, and Computer Modelling and New Technologies. Editor in Chief of the MDPI journal "Materials" in the Section Board for 'Carbon Materials'

He is Director of the NATO Emerging Security Challenges Division, SPS Programme projects "Nanocomposite based photonic crystal sensors of biological and chemical agents," "Development of Biosensors using Carbon Nanotubes". He is INFN scientist in charge of EU project "Graphene-Based Revolutions in ICT And Beyond, GRAPHENE Flagship" Core1, and INFN scientist in charge of Italy Ministry of Health project "Delivery and imaging of miRNAs by multifunctional carbon nanotubes and circulating miRNAs as innovative therapeutic and diagnostic tools for pediatric pulmonary hypertension" and of Italy Space Agency project "SHAPE- A New Theoretical Framework of the Microgravity-Cell Interaction". He is LNF Spokesperson of NEMESYS Condensed Matter Theory INFN CSN4 project.